Journal of Molecular Graphics and Modelling 69 (2016) 92–102

Contents lists available at ScienceDirect

Journal of Molecular Graphics and Modelling

journal homepage: www.elsevier.com/locate/JMGM

Mutagenicity of heteroaromatic amines: Computational study on the influence of methyl substituents

Gabriela L. Borosky

INFIQC, CONICET and Departamento de Matemática y Física, Facultad de Ciencias Químicas, Universidad Nacional de Córdoba, Ciudad Universitaria, Córdoba 5000, Argentina

ARTICLE INFO

Article history:
Received 28 July 2016
Received in revised form 18 August 2016
Accepted 27 August 2016
Available online 28 August 2016

Keywords:
Heteroaromatic amines
Mutagenicity
DNA adducts
Quantum chemistry
Noncovalent interactions

ABSTRACT

Quantum mechanical calculations were performed to elucidate the factors determining the variations in mutagenic activity within groups of isomeric heteroaromatic amines that differ in the position of methyl substituents. Formation energies for noncovalent complexes and covalent DNA adducts were evaluated by means of high level quantum chemical methods. According to the computational results in this work, covalent adduct stability is proposed to influence the relative mutagenicities of structurally related heterocyclic amines. The stability of covalent C8-dG DNA adducts was found to be mainly determined by π-stacking interactions between the fused ring system of the heteroaromatic amines and the flanking nucleobases. Relative mutagenicity of amines of very related structure is proposed to be regulated by both nitrenium ion and covalent adduct stabilities.

1. Introduction

Arylamines have broad utilization in textile, plastic, cosmetic, food, and pharmaceutical industries, and are well-known environmental carcinogens [1–4]. Heterocyclic aromatic amines present in cooked meats and protein rich foods have also been determined to be mutagenic and carcinogenic [5–9]. These compounds require enzymatic metabolic activation in order to exert its genotoxic potential [10–13]. The main mutagenic pathway initiates with oxidation of the exocyclic amine nitrogen to form aryl *N*-hydroxylamines [10,13], which can undergo N—O bond cleavage to arylnitrenium ions under mildly acidic conditions [12]; bioactivation of *N*-hydroxylamines to *N*-sulfate or *N*-acetoxy esters further assists the heterolysis of the N—O bond [10–12]. This process produces electrophilic and highly reactive nitrenium ions as the ultimate metabolites that covalently modify nucleic bases of DNA, primarily guanines [3,10–12,14]. Replication of covalent DNA adducts may lead to mutations able to cause cancer [14–16].

The relative stability of nitrenium intermediates has been pointed out as a determining factor for bioactivity of aromatic amines [10]. In earlier theoretical studies employing semi-empirical methods, mutagenicity was proposed to increase with the stability of the derived nitrenium ions [17–19]. Formation of these electrophilic intermediates from their precursors was later examined by more accurate density functional theory (DFT) computations [20,21]. Good correlations were observed for a wide range of experimental values of mutagenic potencies with calculated reaction energies and electronic properties for series of structurally related aromatic and heteroaromatic amines, indicating that mutagenic activity increased with nitrenium ion stability [20,21]. Afterwards, DFT calculations were successfully applied in several studies aimed to relate mutagenicity with the stability of the corresponding nitrenium ions [22–28].

Nitrenium stability was shown to improve with the number of aromatic rings (resonance effect) and with methyl substitution (hyperconjugative and inductive effects) [21]. In contrast, the stability of the corresponding nitrenium cations did not follow the mutagenicity order for some pairs of amines differing in the number or position of the methyl groups [21]. Nevertheless, bioactivity is triggered via complex processes and should be influenced by several factors, such as solubility, transport, specific interactions within the enzymes involved in the activation pathway, and DNA intercalation.

Nitrenium ions preferably react with deoxyguanosine (dG) nucleobases of DNA, the C8 position of guanine being the primary target for covalent adduct formation [11,14,29]. By using 9-methylguanine as a model of dG, recent theoretical studies have

E-mail address: gborosky@fcq.unc.edu.ar

http://dx.doi.org/10.1016/j.jmgm.2016.08.010
1093-3263/

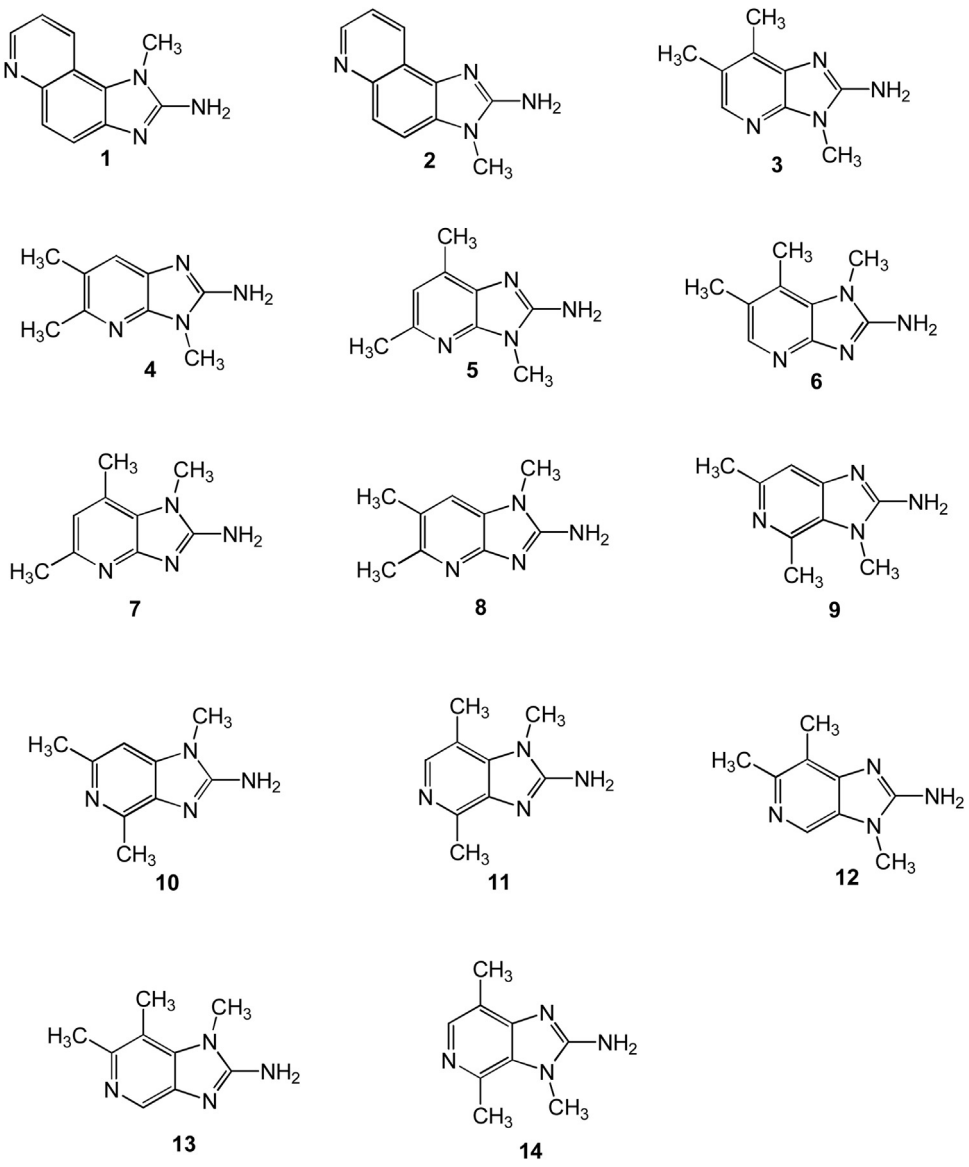

Fig. 1. Heteroaromatic amines studied.

proposed that the mutagenic potency of aromatic and heteroaromatic amines correlates with the rate of formation of the nitrenium ions and with their chemical reactivity toward the C8 atom of guanine to form C8-dG DNA adducts [30]. Molecular mechanics calculations for a double-stranded oligonucleotide $(dG)_{20}/(dC)_{20}$ suggested that precovalent DNA intercalation is not an essential step for genotoxicity of these compounds [30]. The importance of the covalent binding step on the mutagenicity of heterocyclic aromatic amines was lately pointed out by semi-empirical PM3 computations of the stability of C8-dG DNA adducts, employing a DNA model with three base pairs [31]. The interaction between methyl substituents in the amine with phosphate groups in DNA was indicated to play a significant role in the stabilization of the amine-DNA covalent adducts [31].

In this work, groups of isomeric heteroaromatic amines structurally related, differing only in the position of methyl substituents (Fig. 1), were selected to study the influence of methyl substitution on structure-mutagenicity relationships. With the aim of achieving a better understanding of the role of DNA intercalation and covalent adduct formation on the genotoxicity of aromatic amines, these processes were investigated by means of high level quantum mechanical calculations.

2. Computational methods

2.1. Docking procedure

Preliminary molecular docking calculations were carried out in order to obtain initial structures for noncovalent complexes. Three-dimensional coordinates of double stranded B-DNA dodecamers were obtained from the Protein Data Bank (PDB codes 2Z2G [32] and 2HKC [33], which are C8-dG covalent adducts of the heterocyclic amine 2-amino-3-methylimidazo[4,5-*f*]quinoline (IQ); and the corresponding unmodified B-DNA sequence 2HKB [33]). The programs AutoDock 4.2 [34] and AutoDock Vina [35] were utilized to carry out automated molecular docking for estimating the interaction energy and modeling the binding modes between the DNA duplexes and the nitrenium ions. The IQ ligand was removed, and the resulting valence at guanine was completed with a hydrogen atom. Gasteiger partial charges were assigned to atoms and non-

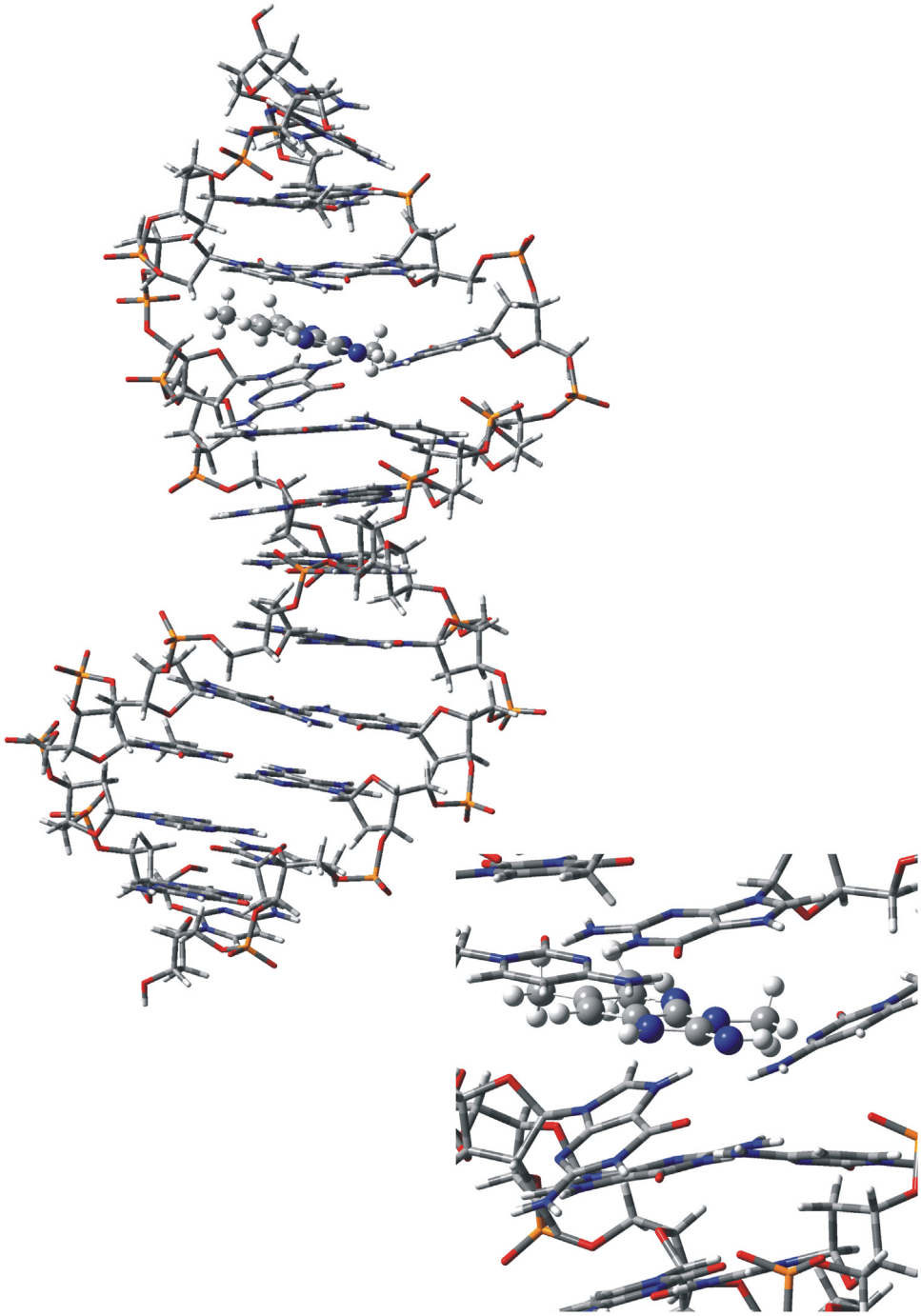

Fig. 2. Best docked conformation for a representative nitrenium ion.

polar hydrogens were merged to the atom to which they were attached with AutoDockTools. The docking area was defined using the AutoDock module AutoGrid. The grid box was constrained to 26.2 Å in the x- and y-dimensions and 39.0 Å in the z-dimension, centered at the DNA solution structure [32,33] and comprising the entire duplex. The orientational space of the ligands was searched within the rigid DNA structure. With AutoDock 4.2, the Lamarckian genetic algorithm (LGA) was used, default parameters were applied, and the maximum number of energy evaluations was set to 1.0×10^7. For each of the 100 independent runs performed for each nitrenium ligand, a maximum number of 2.7×10^4 genetic algorithm operations were generated on a single population of 150 individuals. Operator weights for crossover, mutation, and elitism were default parameters, 0.80, 0.02, and 1, respectively. Default parameters were also used for Vina.

2.2. Quantum-mechanical methods

Calculations were performed with the Gaussian 09 package of programs [36]. The relative stability of nitrenium ions was computed at the B3LYP/6-31G* level [37–39], and natural bond orbital population analysis (NPA) was evaluated at the same level by the NBO program [40]. The composite method CBS-QB3 [41] was also applied to obtain more accurate relative stabilities for nitrenium ions. A two-layer QM/QM-ONIOM [42] approach was employed to carry out quantum-mechanical geometry optimiza-

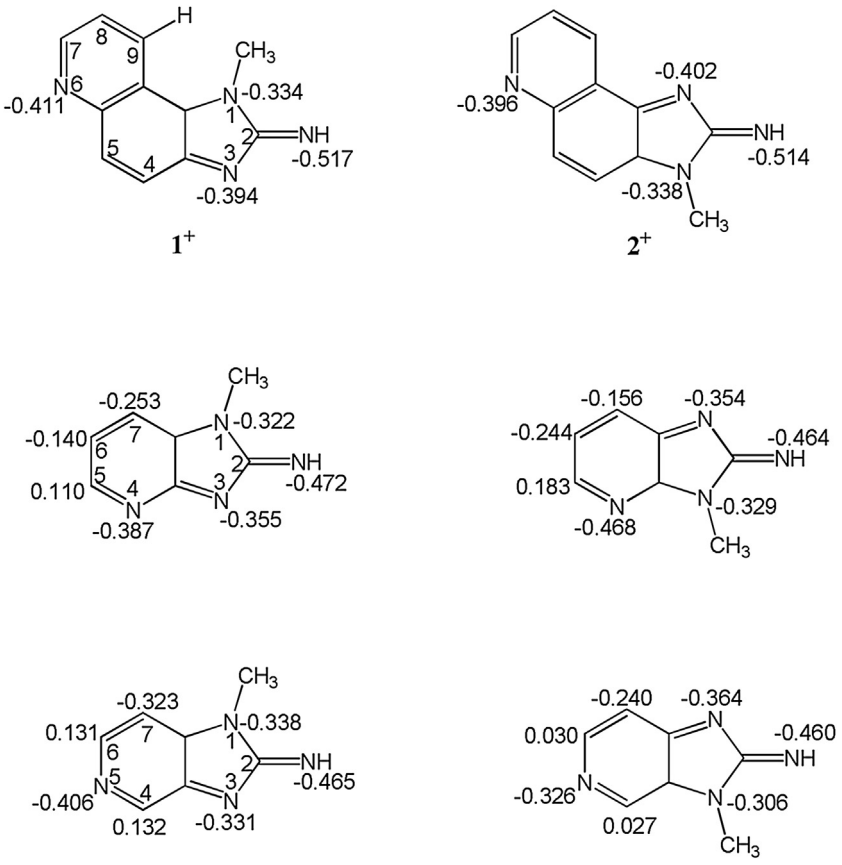

Fig. 3. NPA charge density distribution for selected nitrenium ions.

tions for noncovalent complexes and covalent amine-DNA adducts. The lowest energy pose of the best docked productive complex for each compound was used to build the initial data for the noncovalent complexes. The initial geometry for the covalent adducts was constructed using two different IQ-DNA adducts as templates (PDB codes 2Z2G [32] and 2HKC [33]). The employed DNA polynucleotide consisted of five pairs of complementary bases with their corresponding ten sugar units (deoxyribose) and ten deprotonated phosphate groups. DFT calculations were performed with the ωB97X-D functional [43], which includes empirical dispersion, in order to attain a proper description of π-π stacking interactions between adjacent DNA base pairs. Geometry optimizations at the ωB97X-D/6-31G* level were carried out for the high layer, which comprised the interacting entities, *i.e.*, the nitrenium ions and the reacting central guanine with its opposite cytosine base. For the rest of the atoms (low layer) the PM6 semi-empirical method was applied [44]. The DNA double-helix structure was retained by fixing the coordinates of the phosphate groups, and the sugar atoms to which they were linked, while the coordinates of all the other atoms were fully optimized. It should be noted that calculations without these geometrical restrictions lead to a pronounced distortion of the model. The effect of the environment within the minor groove of DNA was estimated by energy minimizations employing the polarized continuum model IEFPCM [45–48] (QM/QM-ONIOM(ωB97X-D/6-31G*:PM6)-PCM). Based on the characterization of the minor groove environment in a drug-DNA complex [49], the dielectric constant of the model was set to a value $\varepsilon = 20$.

3. Results and discussion

Carcinogen-DNA covalent adducts can produce mutations during DNA replication, especially when occurring in a hot spot, and mutations in protein coding regions may ultimately lead to cancer [14–16]. The 5′-d(CG^{1}G^{2}CG^{3}CC)-3′ recognition sequence of the *Nar*I restriction enzyme in *E. coli* represents the strongest known hot spot for frameshift mutagenesis [50,51]. Considering this, the NMR solution structure of a C8-dG adduct of the heteroaromatic amine IQ in this sequence was selected from the Protein Data Bank (PDB code 2Z2G) [32]. In this adduct the IQ moiety was oriented in the minor groove, and the double helix base pairing and B-DNA structure were less altered than in base-displaced intercalated adduct conformations. After deleting the covalently bonded IQ, the dodecamer 5′-d(CTCGGCGCCATC)-3′·5′-d(GATGGCGCCGAG)3′ was employed as receptor for performing preliminary molecular docking calculations, with the aim of obtaining initial structures for noncovalent complexes.

Both neutral amines and nitrenium ions were used as ligands in the docking studies. A greater interaction of the nitreniums with the region of the DNA lesion was observed, as their docked conformations were better positioned for subsequent reaction with the adducted guanine of the PDB structure (Fig. 2). AutoDock 4.2 and AutoDock Vina afforded similar results, with binding energies around −6 kcal/mol for the nitrenium ions in the 2Z2G duplex. The unmodified *Nar*I duplex (PDB code 2HKB [33]) was also utilized as receptor, but the resulting docking poses (noncovalent complexes) were less orientated to form covalent adducts when the base pairs were in the canonical intact orientation.

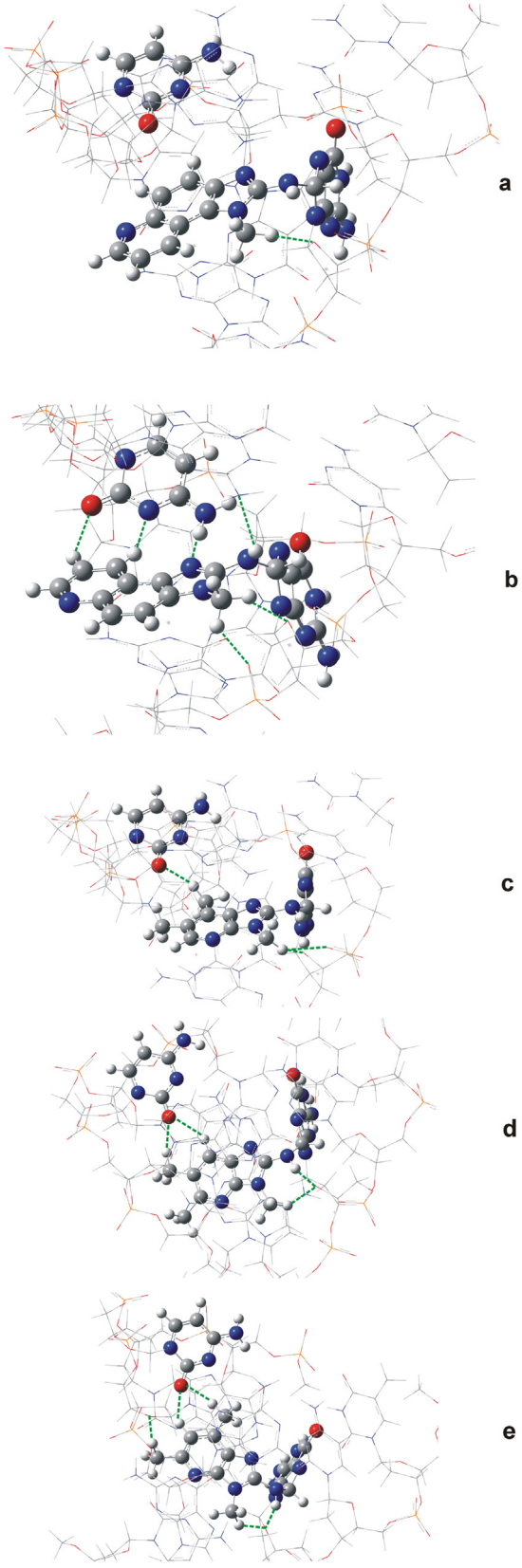

Fig. 4. Protonated covalent adducts for nitrenium ions (H-bonding contacts are indicated by green dashed lines): a) $\mathbf{1}^+$; b) $\mathbf{2}^+$; c) $\mathbf{3}^+$; d) $\mathbf{4}^+$; e) $\mathbf{5}^+$.

Within the 5′-d(CG[1]G[2]CG[3]CC)-3′ *Nar*I sequence, the propensity for −2 bp frameshifts is sequence-dependent, and these mutations only occur following adduct formation at the G[3] position [51–53]. Considering this fact, the NMR solution structure of the C8-dG IQ modified *Nar*1IQ3 duplex was obtained from the Protein Data Bank (PDB code 2HKC) [33]. In this base-displaced intercalated adduct the adducted dG extrudes into the major groove, the IQ moiety intercalates into the DNA flanking base pairs, and the complementary dC extrudes from the helix into the major groove. Upon deletion of the covalently bonded IQ, this dodecamer was also employed as receptor in molecular docking calculations, but binding energies were slightly less favorable than with the 2Z2G duplex. Consequently, the docking modes obtained with 2Z2G were used as initial structures for the subsequent quantum-mechanical optimizations of noncovalent complexes.

For the quantum-chemical computations, the system under study consisted of sets of heterocyclic amines that present the same molecular structure and only differ in the methyl substitution sites (compounds **1** and **2** (IQ), 2-amino-trimethylimidazo[4,5-*b*]pyridines **3**-**8**, and 2-amino-trimethylimidazo[4,5-*c*]pyridines **9**-**14**, Fig. 1). Nitrenium ion relative stabilities, estimated by the change in energy for Reaction 1, were computed at the B3LYP/6-31G* level and with the more accurate CBS-QB3 composite method, both procedures affording nearly the same relative stability trend. The relative stabilities of the derived nitrenium ions within each group were very similar, and did not explain the observed differences in mutagenic activity (logMP) (Table 1).

$$ArNH_2 \xrightarrow{-H^-} ArNH^+ \quad (1)$$

The higher stability of nitrenium $\mathbf{2}^+$ in comparison with $\mathbf{1}^+$ relies on the greater delocalization of the total positive charge with methyl substitution at N3. This can be assessed by small modifications observed in the bond lengths within the heteroaromatic six-membered ring, and by the lower negative charge density at the ring nitrogen atoms, especially N6 (Fig. 3). Besides, methylation at N1 led to a slight distortion of the aromatic system angles in order to minimize steric repulsions between C9-H and the methyl group hydrogens.

The relative stability of the nitrenium ions derived from the 2-amino-trimethylimidazopyridine isomers can be ascribed to the charge density distribution in the nitreniums of the parent compounds (Fig. 3). In this way, the stability order $\mathbf{5}^+ > \mathbf{4}^+ > \mathbf{3}^+$ (methylated at N3) is explained by the charge distribution at positions 5, 6, and 7, which is best stabilized by methylation at C5 > C7 > C6. Similarly, the charge density at C5, C6, and C7 determines the stability of $\mathbf{8}^+ > \mathbf{7}^+ > \mathbf{6}^+$ (methylated at N1). Considering the other two sets (2-amino-trimethylimidazo[4,5-*c*]pyridines), preferred methylation at C4 and C6 accounts for the stability of $\mathbf{9}^+ > \mathbf{12}^+ \approx \mathbf{14}^+$, as well as for $\mathbf{10}^+ > \mathbf{11}^+ \approx \mathbf{13}^+$.

The formation of C8-dG adducts was examined by ONIOM(ωB97X-D/6-31G*:PM6)-PCM computations. The nitrenium ions derived from the heterocyclic amines in Fig. 1 were allowed to interact with a double-stranded DNA polynucleotide, consisting of five complementary base pairs (5′-d(TCGGC)-3′·5′-d(GCCGA)3′, extracted from the PDB code 2Z2G [32]), to form a noncovalent complex in a first step. The C8-protonated amine-DNA covalent adducts with the central guanine were subsequently modeled. Cationic C8 intermediates result in C8 guanine adducts after proton loss [30]. Results are displayed in Table 1, where reported changes in energy were calculated by the following Equations:

$$\Delta E_{NC} = E_{\text{noncovalent complex}} - E_{\text{nitrenium}} - E_{DNA} \quad (1)$$

$$\Delta E_{CC} = E_{\text{covalent complex}} - E_{\text{noncovalent complex}} \quad (2)$$

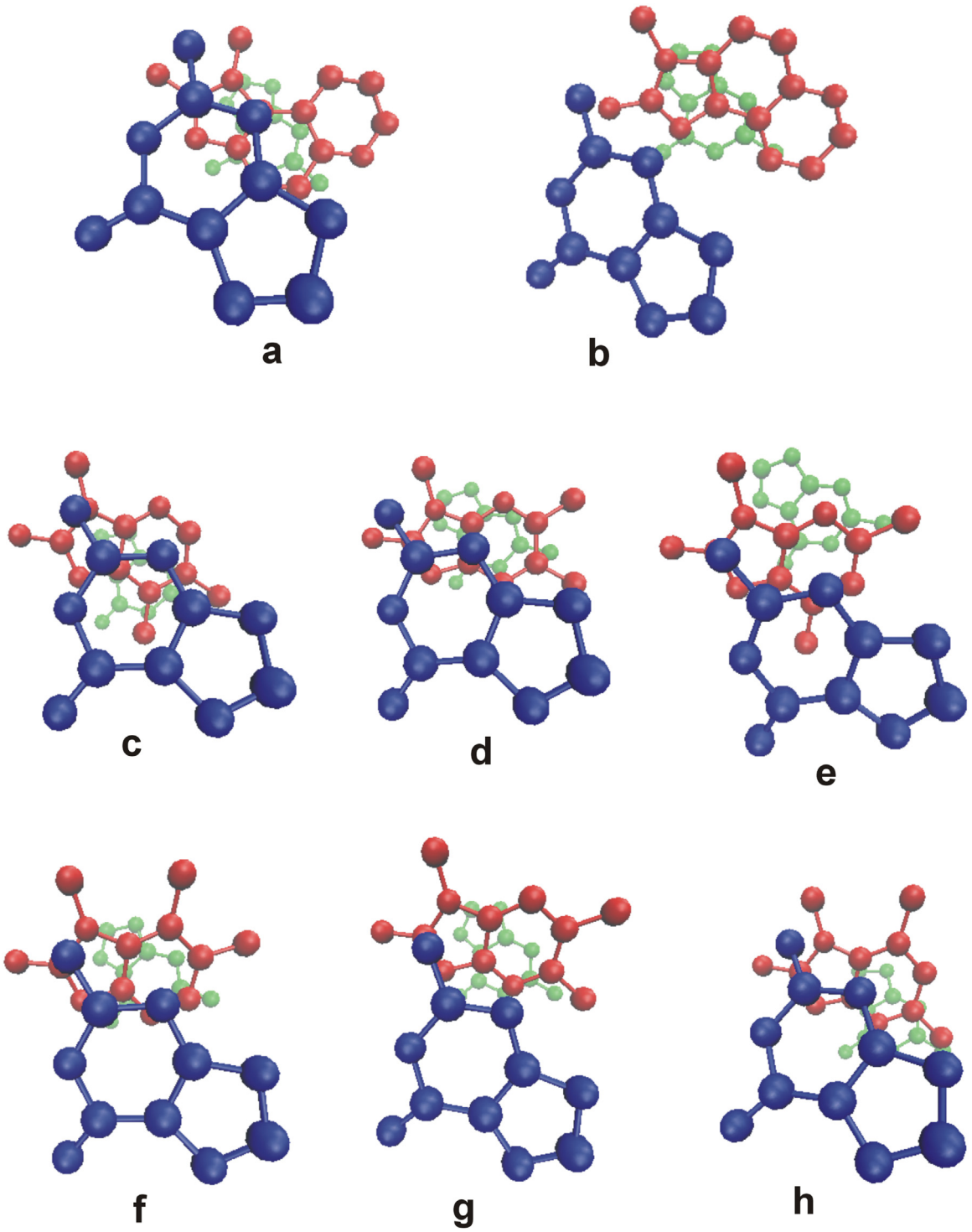

Fig. 5. Stacking interactions of the adducted nitrenium ions (depicted in red) with the neighboring nucleobases (shown in blue and green): a) $\mathbf{1}^+$; b) $\mathbf{2}^+$; c) $\mathbf{3}^+$; d) $\mathbf{4}^+$; e) $\mathbf{5}^+$; f) $\mathbf{6}^+$; g) $\mathbf{7}^+$; h) $\mathbf{8}^+$.

$$\Delta E_{\infty CC} = E_{\text{covalent complex}} - E_{\text{nitrenium}} - E_{DNA} \quad (3)$$

$$\Delta E_{\infty CC'} = E_{\text{covalent complex}} - E_{\text{nitrenium}} - E_{DNA'1(2HKC)} \quad (4)$$

According to data in Table 1, the change in total energy for noncovalent complex formation from the separated reactants (nitrenium ion and polynucleotide at infinite distance) was similar for all the cations, with values around −30 kcal/mol. On the other hand, a correlation between the change in energy for formation of the covalent adduct from the noncovalent complex and mutagenicity was found for the groups of cations $\mathbf{1}^+$ and $\mathbf{2}^+$, $\mathbf{3}^+$–$\mathbf{5}^+$, and $\mathbf{6}^+$–$\mathbf{8}^+$. The same trend was observed when the change in total energy from the separated reactants to the covalent adduct was considered. Hence, the stability of the covalent adducts could be inferred as a factor determining the mutagenic activity.

For nitrenium ions $\mathbf{1}^+$ and $\mathbf{2}^+$, the calculated covalent adduct formation energy was 10 kcal/mol more favorable for the more mutagenic derivative **1** (Table 1). The relative stability of this pair of adducts was rationalized by analyzing the noncovalent interac-

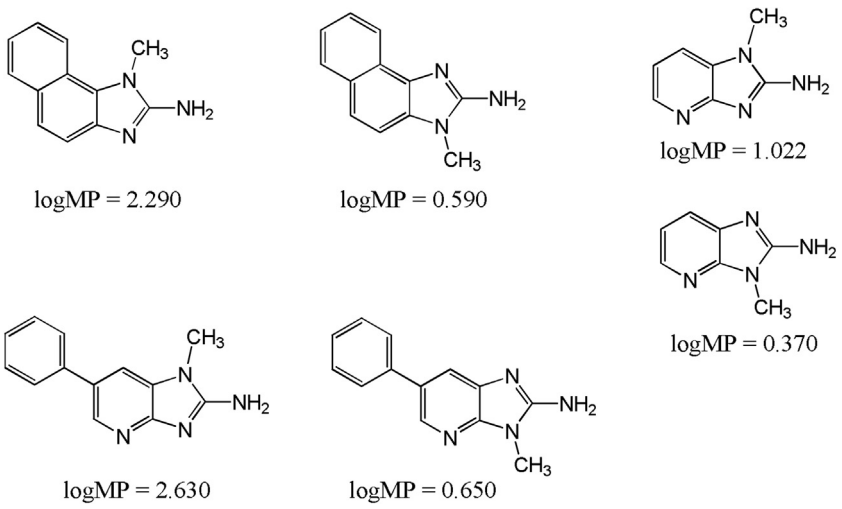

Fig. 6. Mutagenic potencies for other related heteroaromatic amines.

Table 1
Mutagenic potencies and calculated parameters for the studied amines (kcal/mol).

Nitrenium	LogMP[a]	ΔE_{r1}[b]	ΔE_{NC}[c]	ΔE_{CC}[d]	$\Delta E_{\infty CC}$[e]	$\Delta E_{\infty CC'}$[f]
1$^+$	5.790	227.2 (265.3)	−26.9	−21.3	−48.2	–
2$^+$	4.700	226.0 (263.6)	−27.6	−10.2	−37.8	–
3$^+$	1.747	234.8 (274.8)	−29.0	−29.0	−58.0 (−59.2)	−40.7
4$^+$	1.613	231.5 (271.0)	−30.6	−25.1	−55.6 (−59.3)	−40.7
5$^+$	0.693	232.0 (270.2)	−33.3	−20.2	−53.5 (−57.3)	−38.3
6$^+$	0.200	233.9 (274.4)	−28.6	−27.4	−56.1 (−59.2)	−42.2
7$^+$	0.002	234.0 (273.3)	−28.9	−23.6	−52.5 (−58.4)	−45.8
8$^+$	−0.263	231.8 (271.1)	−29.9	−19.8	−49.6 (−55.6)	−42.6
9$^+$	−0.392	241.5 (281.4)	–	–	−65.9	−47.8
10$^+$	−0.550	235.1 (272.7)	–	–	−55.8	−43.1
11$^+$	−0.800	238.1 (277.2)	–	–	−59.7	−47.1
12$^+$	−1.055	243.2 (283.8)	–	–	−67.2	−49.2
13$^+$	−1.055	237.2 (277.0)	–	–	−61.4	−44.7
14$^+$	–	242.8 (283.3)	–	–	−64.4	−52.3

[a] From Refs. [57] and [58].
[b] Change in energy for Reaction 1 at the CBS-QB3 level (B3LYP/6-31G* results in parenthesis).
[c] Change in energy for noncovalent complex formation.
[d] Change in energy for covalent adduct formation (from the noncovalent complex).
[e] Change in energy for covalent adduct formation (from reactants at infinite distance; results with an extended high layer in parenthesis).
[f] Change in energy for covalent adduct formation (considering PDB 2HKC (base-displaced); from reactants at infinite distance).

Table 2
Geometrical parameters for hydrogen bonds and π-stacking interactions in amine-DNA covalent adducts.

Nitrenium	LogMP[a]	$\Delta E_{\infty CC}$ (kcal/mol)[b]	π-Stacking (Å)[c]	Hydrogen bonds (Å)		
				CH_3	NH	CH/N,O
1$^+$	5.790	−48.2	+++ (3.95; 4.08)	2.058		
2$^+$	4.700	−37.8	++ (4.08; 5.20)	2.051; 2.126	2.439	2.384; 2.284; 2.160
3$^+$	1.747	−58.0 (−59.2)	+++ (4.32; 4.57) [4.12; 4.24]	2.353; 2.429; 2.180		
4$^+$	1.613	−55.6 (−59.3)	+++ (4.12; 4.32) [3.67; 3.87]	2.179; 2.299	2.257	2.488
5$^+$	0.693	−53.5 (−57.3)	++ (3.73; 4.70) [3.61; 4.10]	2.099; 2.198; 2.320	2.090	2.213
6$^+$	0.200	−56.1 (−59.2)	+++ (4.20; 4.45) [3.80; 3.89]	2.135; 2.376; 1.993	2.169	
7$^+$	0.002	−52.5 (−58.4)	++ (4.44; 4.51) [3.56; 4.04]	2.324; 2.152; 2.082; 2.475		
8$^+$	−0.263	−49.6 (−55.6)	+ (4.40; 5.11) [3.68; 4.05]	2.241; 2.246; 2.241; 2.405; 2.259; 2.157	2.175	
9$^+$	−0.392	−65.9	+++ (3.81; 4.28)	2.100; 2.276	2.341	
10$^+$	−0.550	−55.8	+++ (4.19; 4.35)	2.214; 2.249; 2.252	2.214	
11$^+$	−0.800	−59.7	+++ (4.17; 4.40)	2.168; 2.288	2.216	
12$^+$	−1.055	−67.2	+++ (4.37; 4.53)	2.238; 2.246: 2.185	2.200	
13$^+$	−1.055	−61.4	+++ (3.91; 4.25)	2.077	2.282	
14$^+$	–	−64.4	+++ (3.91; 4.52)	2.150; 2.469; 2.273; 2.360; 2.286	2.261	

[a] From Refs. [57] and [58].
[b] Change in energy for covalent adduct formation (from separated reactants; extended high layer results in parenthesis).
[c] +++ stronger; ++ medium; + weaker (see text). Smallest distances between ring centroids of the nitrenium moiety and both flanking nucleobases in parenthesis; extended high layer results in square brackets.

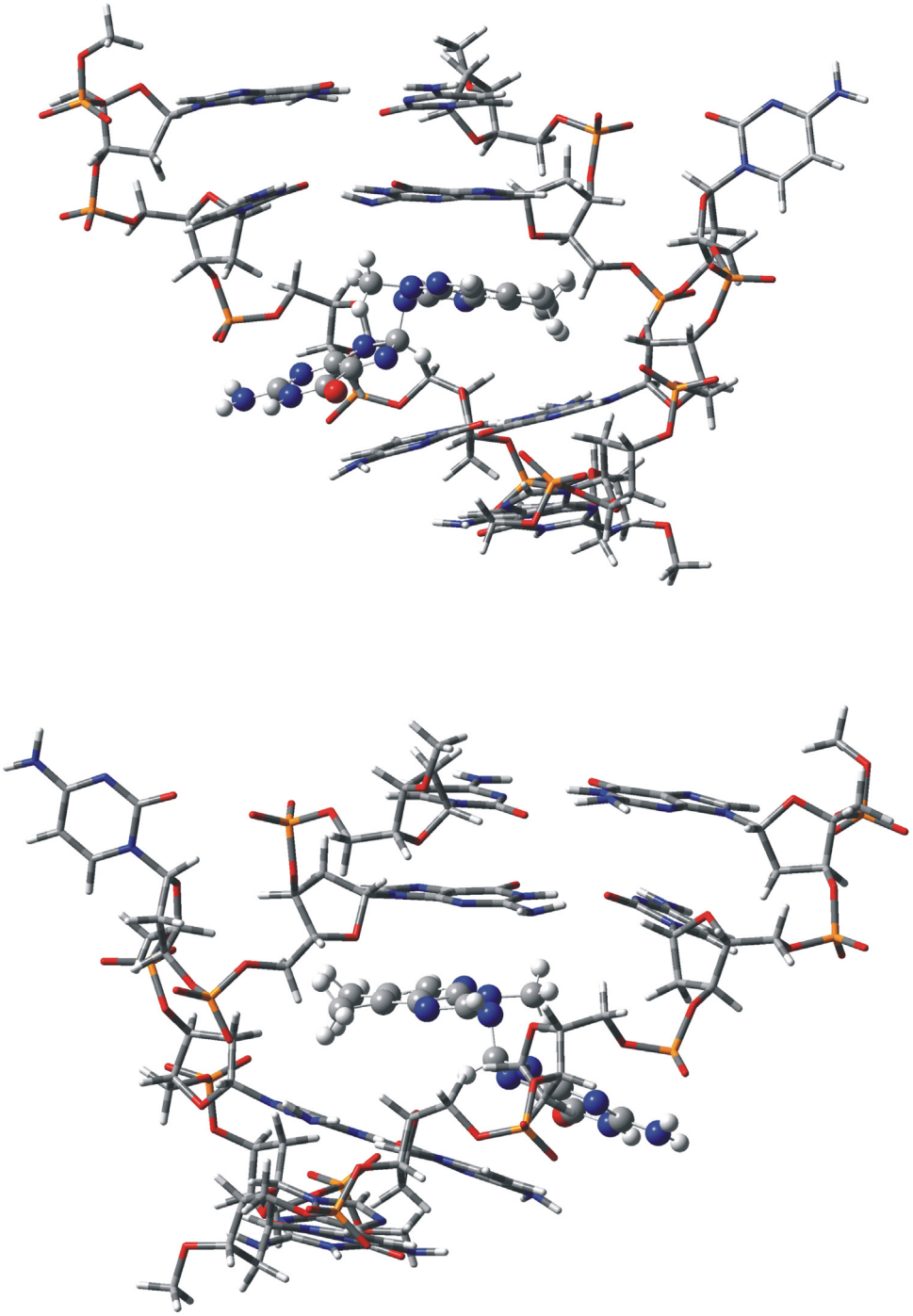

Fig. 7. Two different views of a base-displaced intercalated adduct.

tions between the respective amine moieties and the DNA double helix environment (Table 2). The 1-methyl group in compound **1** formed only one hydrogen bond interaction [54] with the oxygen atom of a vicinal deoxyribose (O—H distance was 2.058 Å). In contrast, the 3-methyl substituent in compound **2** attained two stabilizing hydrogen bonds: one with a deoxyribose (O—H distance was 2.051 Å), and another with an oxygen atom of a phosphate group (2.126 Å). One additional hydrogen bond was achieved by the N—H group of $\mathbf{2}^+$ and the nitrogen of the exocyclic amino group of an adjacent nucleobase, whilst three hydrogen bond interactions were observed with the opposing cytosine (Fig. 4b, and Table 2). General criteria for hydrogen bonding geometries were considered (H—acceptor distance <2.5 Å, donor-H-acceptor angle >120°) [54,55].

On the other hand, π-stacking interactions were stronger in case of the $\mathbf{1}^+$-adduct, whose fused ring system was more efficiently superimposed with both flanking nucleobases located above and below (Fig. 5); while for the $\mathbf{2}^+$-adduct, the IQ moiety was efficiently stacked with only one of the adjacent bases. The relative strength of these interactions was estimated by considering the degree of superposition (Fig. 5) and the shortest distance between ring centroids for each stacked pair of fused ring systems (Table 2). It has been shown that stacking contributes more to the stability of DNA than H-bonding [56]. In line with this,

the relative stability of the covalent adducts formed by nitrenium ions **1**$^+$ and **2**$^+$ appears to be mainly justified by π-stacking contributions. The same deductions would apply considering the relative mutagenicity of the related aromatic amines 2-amino-1-methylnaphtho[2,1-*d*]imidazole (logMP 2.290) and 2-amino-3-methylnaphtho[2,1-*d*]imidazole (logMP 0.590) [57]. It is worth of noticing the higher mutagenicity of the 1-methyl derivatives in comparison with the corresponding 3-methyl compounds that was also assessed for the 2-amino-methylimidazo[4,5-*b*]pyridines and the 2-amino-methyl-6-phenylimidazo[4,5-*b*]pyridines (Fig. 6) [57].

In the **3**$^+$-adduct, the methyl substituents formed two hydrogen bonds with a neighboring deoxyribose (2.353 Å) and a phosphate group (2.429 Å), whereas one more H-bonding interaction (2.180 Å) was attained with the opposite cytosine base. For the **4**$^+$-adduct, four H-bonds were formed (2.179, 2.257, 2.299, and 2.488 Å); and in case of the **5**$^+$-adduct, five H-bonds were observed (see Table 2 and Fig. 4e for details). On the basis of superimposition extent and distance, π-stacking interactions with the nucleobases placed above and below followed the strength order **3**$^+$-adduct ≥ **4**$^+$-adduct > **5**$^+$-adduct, which matches with covalent adduct stability and mutagenic potency (Table 2 and Fig. 5).

For covalent adducts of nitrenium ions **6**$^+$, **7**$^+$ and **8**$^+$, the largest number of hydrogen bond interactions was observed for the less mutagenic amine **8**; whereas π-stacking interactions were **6**$^+$-adduct > **7**$^+$-adduct » **8**$^+$-adduct, in good correspondence with covalent adduct stability and mutagenic potency (Table 2 and Fig. 5).

For the imidazo[4,5-*c*]pyridine compounds, the relative importance of π-stacking and H-bonding on the resulting covalent adduct stabilities was less evident (Table 2). However, when considering the ions methylated at N3 (**9**$^+$ and **12**$^+$), and the set methylated at N1 (**10**$^+$, **11**$^+$ and **13**$^+$), an inverse correlation was observed between the relative stability of the covalent adducts and logMP. Instead, for these derivatives mutagenic potency appeared to be related with nitrenium ion stability. These structures, which correspond to the less stable nitrenium ions in Table 1, are also the less mutagenic. It should be noted that synthesis efforts aimed to make amine **14** available for mutagenicity studies were not successful [58]. According to the computed relative stability of **14**$^+$, its mutagenic activity would be expected to be similar to compound **12**.

An additional DNA model with an extended DFT high layer, which included both nucleobases flanking the heteroaromatic amine rings, was also considered in order to get a better description of the π-stacking interactions involved. Geometry optimizations of the covalent adducts for nitrenium ions **3**$^+$-**8**$^+$ were carried out with this improved model. The distance between superimposed aromatic rings involved in π-stacking interactions decreased, in concert with the enhancement in the stability of the resulting adducts with respect to the separated reactants (Table 2). These observations support the importance of π-stacking on the stability of the covalent adducts.

Relative covalent adduct stability seemed to be more influential on mutagenic potency when comparing nitrenium ions of very similar stability, as for example, in case of cations **1**$^+$ and **2**$^+$. While **2**$^+$ is more stable by around 1 kcal/mol, and would therefore be expected to be more mutagenic than **1**$^+$ [17–28], the 12.3 times greater mutagenicity of the latter can be ascribed to the 10 kcal/mol higher stability of the **1**$^+$-adduct. On the other hand, whereas the **6**$^+$-adduct is relatively more stable than those formed by **4**$^+$ and **5**$^+$, the lower stability of **6**$^+$ in relation to the two other cations justifies its lower bioactivity. Nitreniums **3**$^+$ and **6**$^+$ present similar stability, but formation of the **3**$^+$-adduct is more favorable and determines the mutagenicity order; the same observations apply when comparing **8**$^+$ and **4**$^+$. In this way, the present results suggest that an interplay between nitrenium and adduct stabilities rules mutagenicity for amines of very related structure. The relative mutagenic potency between each pair of consecutive rows in Table 1 can be accounted for by one of these two criteria.

Within the 5′-d(CG^{1}G^{2}CG^{3}CC)-3′ *Nar*I sequence, mutations only occur following adduct formation at the G^3 position [51–53]. Considering this, formation of the corresponding C8-dG^3 covalent adducts was also evaluated by employing a duplex consisting of five complementary base pairs extracted from the PDB code 2HKC [33] (G^3 at the central base pair). In these base-displaced intercalated adducts, the adducted dG^3 and its opposite dC extruded from the helix into the major groove (Fig. 7). But in this case, no correlation was observed between the change in energy for adduct formation and mutagenicity (Table 1). This distorted intercalated conformation could be adopted following initial adduct formation in the less altered form described above (with the adducted carcinogen placed in the minor groove, based on the 2Z2G structure). Subsequent deformation of the DNA helix to achieve a base-displaced structure could hinder cellular repair pathways, thus leading to mutations. Mutagenesis involves a balance between the efficiencies of DNA repair systems and polymerases, which action is influenced by the conformational nature of aromatic amine adducts [14].

4. Summary and conclusions

The initial noncovalent intercalation modes of nitrenium ions derived from heteroaromatic amines within a double-stranded DNA polynucleotide were analyzed, and subsequent formation of C8-dG DNA covalent adducts was evaluated. The change in energy for noncovalent complex formation from the separated reactants was similar for all the cations considered. On the other hand, a correlation between the change in energy for formation of covalent adducts and mutagenicity was observed within groups of amines differing only in the position of methyl substituents.

Covalent adduct stability appeared to be more determined by π-stacking interactions between the heteroaromatic amine rings and the flanking nucleobases, than by H-bonding contributions. It should be noticed that no CH-π interactions between the methyl groups and the adjacent base pairs were observed for the methylamines studied. The influence of methyl substituents on mutagenicity, related with amine-DNA covalent adduct stability, would therefore be linked with the formation of stabilizing hydrogen bonds. More importantly, methyl substitutions that sterically disrupt π-stacking interactions between the amine aromatic rings and vicinal nucleobases of the DNA helix would lead to a decrease in mutagenic potency.

Bioactivity of chemical carcinogens generally involves a complex set of metabolic processes, and is affected by several aspects such as solubility, transport, DNA repair mechanisms, translesion replication, and specific interactions with the biological environment. According to the present theoretical results, the stability of the corresponding covalent adducts with DNA is pointed to as an additional aspect influencing the mutagenicity of heteroaromatic and aromatic amines. Thus, both nitrenium ion and covalent adduct stabilities are proposed to affect relative mutagenicity when considering amines of very related structure.

Acknowledgements

The author gratefully acknowledges financial support from Consejo Nacional de Investigaciones Científicas y Técnicas (CONICET) and the Secretaría de Ciencia y Tecnología de la Universidad Nacional de Córdoba (Secyt-UNC). This work used Mendieta and Cristina Clusters from CCAD-UNC, which is part of SNCAD-MinCyT, Argentina.

Appendix A. Supplementary data

Supplementary data associated with this article can be found, in the online version, at http://dx.doi.org/10.1016/j.jmgm.2016.08.010.

References

[1] R.C. Garner, C.N. Martin, D.B. Clayson, Carcinogenic aromatic amines and related compounds. In Chemical Carcinogens; Searle, C. E., Ed.; American Chemical Society: Washington, DC, American Chemical Society Monogr., 182, Vol. 1 (1982) pp 175–276.
[2] D.W. Later, R.A. Pelroy, D.L. Stewart, T. McFall, G.M. Both, M.L. Lee, M. Tedjamulia, R.N. Castle, Microbial mutagenicity of isomeric two-, three, and four-rings amino polycyclic aromatic hydrocarbons, Environ. Mutagen. 6 (1984) 497–515.
[3] R.J. Turesky, Aromatic amines and heterocyclic aromatic amines: from tobacco smoke to food mutagens, in: N.E. Geacintov, S. Broyde (Eds.), The Chemical Biology of DNA Damage, Wiley-VCH Verlag, Weinheim, 2010, pp. 157–183.
[4] P.D. Josephy, B. Mannervik, Molecular Toxicology, 2nd ed., Oxford University Press, New York, 2006.
[5] T. Sugimura, K. Wakabayashi, H. Nakagama, M. Nagao, Heterocyclic amines: mutagens/carcinogens produced during cooking of meat and fish, Cancer Sci. 95 (2004) 290–299.
[6] J.S. Felton, M.G. Knize, F.T. Hatch, M.J. Tanga, M.E. Colvin, Heterocyclic amine formation and the impact of structure on their mutagenicity, Cancer Lett. 143 (1999) 127–134.
[7] T. Sugimura, Overview of carcinogenic heterocyclic amines, Mutat. Res. 376 (1997) 211–219.
[8] H.A.J. Schut, E.G. Snyderwine, DNA adducts of heterocyclic amine food mutagens: implications for mutagenesis and carcinogenesis, Carcinogenesis 20 (1999) 353–368.
[9] J.H. Weisburger, Comments on the history and importance of aromatic and heterocyclic amines in public health, Mutat. Res. 506/507 (2002) 9–20.
[10] F.F. Kadlubar, F.A. Beland, Comments on the history and importance of aromatic and heterocyclic amines in public health. In Polycyclic Hydrocarbons and Carcinogenesis, Harvey, R.G., (Ed.) American Chemical Society: Washington, DC, ACS Symposium Series, 283 (1985) pp 341–370.
[11] F.A. Beland, F.F. Kadlubar, Metabolic activation and DNA adducts of aromatic amines and nitroaromatic hydrocarbons, in: C.S. Cooper, P.L. Grover (Eds.), Handbook of Experimental Pharmacology, vol. 94, Springer-Verlag, Heidelberg, 1990, pp. 267–325 (Part 1).
[12] F.F. Kadlubar, J.A. Miller, E.C. Miller, Hepatic microsomal *N*-glucuronidation and nucleic acid binding of *N*-hydroxy arylamines in relation to urinary bladder carcinogenesis, Cancer Res. 37 (1977) 805–814.
[13] D. Kim, F.P. Guengerich, Cytochrome P450 activation of arylamines and heterocyclic amines, Annu. Rev. Pharmacol. Toxicol. 45 (2005) 27–29.
[14] B. Cho, Structure-function characteristics of aromatic amine-DNA adducts, in: N.E. Geacintov, S. Broyde (Eds.), The Chemical Biology of DNA Damage, Wiley-VCH Verlag, Weinheim, 2010, pp. 217–238.
[15] G.R. Hoffmann, R.P.P. Fuchs, Mechanisms of frameshift mutations: insight from aromatic amines, Chem. Res. Toxicol. 10 (1997) 347–359.
[16] S.A. Kulkarni, D. Moir, J. Zhu, Influence of structural and functional modifications of selected genotoxic carcinogens on metabolism and mutagenicity. A review, SAR QSAR Environ. Res. 18 (2007) 459–514.
[17] G.F. Ford, P.S. Herman, Relative stabilities of nitrenium ions derived from polycyclic aromatic amines: relationship to mutagenicity, Chem. Biol. Interact. 81 (1992) 1–18.
[18] G.F. Ford, G.R. Griffin, Relative stabilities of nitrenium ions derived from heterocyclic amine food carcinogens: relationship to mutagenicity, Chem. Biol. Interact. 81 (1992) 19–33.
[19] G. Sabbioni, D. Wild, Quantitative structure-activity relationships of mutagenic aromatic and heteroaromatic azides and amines, Carcinogenesis 13 (1992) 709–713.
[20] G.L. Borosky, Ultimate carcinogenic metabolites from aromatic and heterocyclic aromatic amines: a computational study in relation to their mutagenic potency, Chem. Res. Toxicol. 20 (2007) 171–180.
[21] G.L. Borosky, Carcinogenic carbocyclic and heterocyclic aromatic amines: a DFT study concerning their mutagenic potency, J. Mol. Graph. Model. 27 (2008) 459–465.
[22] A.G. Leach, R. Cann, S. Tomasi, Reaction energies computed with density functional theory correspond with a whole organism effect; modelling the Ames test for mutagenicity, Chem. Commun. (2009) 1094–1096.
[23] J. Bentzien, E.R. Hickey, R.A. Kemper, M.L. Brewer, J.D. Dyekjær, S.P. East, M. Whittaker, An in silico method for predicting Ames activities of primary aromatic amines by calculating the stabilities of nitrenium ions, J. Chem. Inf. Model. 50 (2010) 274–297.
[24] P. McCarren, G.R. Bebernitz, P. Gedeck, S. Glowienke, M.S. Grondine, L.C. Kirman, J. Klickstein, H.F. Schuster, L. Whitehead, Avoidance of the Ames test liability for aryl-amines via computation, Bioorg. Med. Chem. 19 (2011) 3173–3182.
[25] V.M. Arlt, H. Glatt, G. Gamboa da Costa, J. Reynisson, T. Takamura-Enya, D.H. Phillips, Mutagenicity and DNA adduct formation by the urban air pollutant 2-nitrobenzanthrone, Toxicol. Sci. 98 (2007) 445–457.
[26] J. Reynisson, M. Stiborová, V. Martínek, G. Gamboa da Costa, D.H. Phillips, V.M. Arlt, Mutagenic potential of nitrenium ions of nitrobenzanthrones: correlation between theory and experiment, Environ. Mol. Mutagen. 49 (2008) 659–667.
[27] E.J. Kim, A.M. Matuszek, B. Yu, J. Reynisson, Theoretical investigations into the role of aryl nitrenium ions'ı stability on their mutagenic potential, Aust. J. Chem. 64 (2011) 910–915.
[28] A.M. Birch, S. Groombridge, R. Law, A.G. Leach, C.D. Mee, C. Schramm, Rationally designing safer anilines: the challenging case of 4-aminobiphenyls, J. Med. Chem. 55 (2012) 3923–3933.
[29] A. Dipple, DNA adducts of chemical carcinogens, Carcinogenesis 16 (1995) 437–441.
[30] I. Shamovsky, L. Ripa, N. Blomberg, L.A. Eriksson, P. Hansen, C. Mee, C. Tyrchan, M. O'ıDonovan, P. Sjö, Theoretical studies of chemical reactivity of metabolically activated forms of aromatic amines toward DNA, Chem. Res. Toxicol. 25 (2012) 2236–2252 (and references therein).
[31] S. Yamagami, S. Ohshima, Relationship between mutagenicity of heterocyclic aromatic amines and stability of their DNA-adducts: a study by semi-empirical molecular orbital method, Polycyclic Aromat. Compd. 34 (2014) 89–102.
[32] F. Wang, C.E. Elmquist, J.S. Stover, C.J. Rizzo, M.P. Stone, DNA sequence modulates the conformation of the food mutagen 2-amino-3-methylimidazo[4,5- *f*]quinoline in the recognition sequence of the NarI restriction enzyme, Biochemistry 46 (2007) 8498–8516.
[33] F. Wang, N.E. DeMuro, C.E. Elmquist, J.S. Stover, C.J. Rizzo, M.P. Stone, Base-displaced intercalated structure of the food mutagen 2-amino-3-methylimidazo[4,5-*f*]quinoline in the recognition sequence of the NarI restriction enzyme, a hotspot for −2 bp deletions, J. Am. Chem. Soc. 128 (2006) 10085–10095.
[34] G.M. Morris, R. Huey, W. Lindstrom, M.F. Sanner, R.K. Belew, D.S. Goodsell, A.J. Olson, AutoDock4 and AutoDockTools4: automated docking with selective receptor flexibility, J. Comput. Chem. 30 (2009) 2785–2791.
[35] O. Trott, A.J. Olson, Software news and update AutoDock Vina: improving the speed and accuracy of docking with a new scoring function, efficient optimization, and multithreading, J. Comput. Chem. 31 (2010) 455–461.
[36] M.J. Frisch, G.W. Trucks, H.B. Schlegel, G.E. Scuseria, M.A. Robb, J.R. Cheeseman, G. Scalmani, V. Barone, B. Mennucci, G.A. Petersson, et al., Gaussian 09, Gaussian, Inc., Wallingford, CT, 2009.
[37] A.D. Becke, Density-functional thermochemistry: III. The role of exact exchange, J. Chem. Phys. 98 (1993) 5648–5652.
[38] C. Lee, W. Yang, R.G. Parr, Development of the Colle-Salvetti correlation-energy formula into a functional of the electron density, Phys. Rev. B 37 (1998) 785–789.
[39] B. Miehlich, A. Savin, H. Stoll, H. Preuss, Results obtained with the correlation energy density functionals of Becke and Lee, Yang and Parr, Chem. Phys. Lett. 157 (1989) 200–206.
[40] E.D. Glendening, A.E. Reed, J.E. Carpenter, F. Weinhold, NBO Version 3.1, Gaussian, Inc., Wallingford, CT, 2009.
[41] J.A. Montgomery Jr., M.J. Frisch, J.W. Ochterski, G.A. Petersson, A complete basis set model chemistry. VI. Use of density functional geometries and frequencies, J. Chem. Phys. 110 (1999) 2822–2827.
[42] S. Dapprich, I. Komáromi, K.S. Byun, K. Morokuma, M.J. Frisch, A new ONIOM implementation in Gaussian 98. Part I. The calculation of energies, gradients, vibrational frequencies and electric field derivatives, J. Mol. Struct. (Theochem.) 461–462 (1999) 1–21.
[43] J.-D. Chai, M. Head-Gordon, Long-range corrected hybrid density functionals with damped atom–atom dispersion corrections, Phys. Chem. Chem. Phys. 10 (2008) 6615–6620.
[44] J.J.P. Stewart, Optimization of parameters for semiempirical methods V: modification of NDDO approximations and application to 70 elements, J. Mol. Model. 13 (2007) 1173–1213.
[45] E. Cancès, B. Mennucci, J.A. Tomasi, New integral equation formalism for the polarizable continuum model: theoretical background and applications to isotropic and anisotropic dielectrics, J. Chem. Phys. 107 (1997) 3032–3041.
[46] B. Mennucci, J. Tomasi, Continuum solvation models: a new approach to the problem of solute's charge distribution and cavity boundaries, J. Chem. Phys. 106 (1997) 5151–5158.
[47] B. Mennucci, E. Cancès, J. Tomasi, Evaluation of solvent effects in isotropic and anisotropic dielectrics and in ionic solutions with a unified integral equation method: theoretical bases, computational implementation, and numerical applications, J. Phys. Chem. B 101 (1997) 10506–10517.
[48] J. Tomasi, B. Mennucci, E. Cancès, The IEF version of the PCM solvation method: an overview of a new method addressed to study molecular solutes at the QM ab initio level, J. Mol. Struct. (Theochem.) 464 (1999) 211–226.
[49] R. Jin, K.J. Breslauer, Characterization of the minor groove environment in a drug-DNA complex, Proc. Natl. Acad. Sci. U. S. A. 85 (1998) 8939–8942.
[50] D. Burnouf, P. Koehl, R.P.P. Fuchs, Single adduct mutagenesis: strong effect of the position of a single acetylaminofluorene adduct within a mutation hot spot, Proc. Natl. Acad. Sci. U. S. A. 86 (1989) 4147–4151.
[51] T.H. Broschard, N. Koffel-Schwartz, R.P. Fuchs, Sequence-dependent modulation of frameshift mutagenesis at *nar*I-derived mutation hot spots, J. Mol. Biol. 288 (1999) 191–199.

[52] D.Y. Burnouf, R. Miturski, R.P. Fuchs, Sequence context modulation of translesion synthesis at a single *N*-2-acetylaminofluorene adduct located within a mutation hot spot, Chem. Res. Toxicol. 12 (1999) 144–150.
[53] X. Tan, N. Suzuki, A.P. Grollman, S. Shibutani, Mutagenic events in *Escherichia coli* and mammalian cells generated in response to acetylaminofluorene-derived DNA adducts positioned in the narI restriction enzyme site, Biochemistry 41 (2002) 14255–14262.
[54] T. Steiner, Unrolling the hydrogen bond properties of C–H···O interactions, Chem. Commun. (1997) 727–734.
[55] R.E. Hubbard, M.K. Haider, Hydrogen bonds in proteins: role and strength, in: Encyclopedia of Life Sciences (ELS), John Wiley & Sons, Ltd., Chichester, 2010 (and references therein).
[56] K.E. Riley, P. Hobza, Noncovalent interactions in biochemistry, WIREs Comput. Mol. Sci. 1 (2011) 3–17 (and references therein).
[57] F.T. Hatch, M.G. Knize, M.E. Colvin, Extended quantitative structure-activity relationships for 80 aromatic and heterocyclic amines: structural, electronic, and hydropathic factors affecting mutagenic potency, Environ. Mol. Mutagen. 38 (2001) 268–291.
[58] M.G. Knize, F.T. Hatch, M.J. Tanga, E.Y. Lau, M.E. Colvin, A QSAR for the mutagenic potencies of twelve 2-amino-trimethylimidazopyridine isomers: structural, quantum chemical, and hydropathic factors, Environ. Mol. Mutagen. 47 (2006) 132–146.